

LINKING WINDS AND SEDIMENT ACCUMULATION PATTERNS AT HERSCHEL CRATER, MARS.

Brennan W. Young¹, Ryan. C. Ewing², Michael P. Bishop³, Alejandro Soto⁴, Claire E. Newman⁵, Andrew Gunn⁶, Danika N. Martin⁷, and Aviv L. Cohen-Zada⁸, Mathieu G. A. Lapôtre⁹, ¹Texas A&M University Department of Geology & Geophysics (3115 TAMU, College Station, TX 77843-3115, brennan.young@tamu.edu), ²Texas A&M University Department of Geology & Geophysics (College Station, TX, rcewing@tamu.edu), ³Texas A&M University Department of Geography (College Station, TX, michael.bishop@tamu.edu), ⁴Southwest Research Institute (Boulder, CO, asoto@boulder.swri.edu), ⁵Aeolis Research, Chandler, AZ (claire@aeolisresearch.com), ⁶Monash University, School of Earth, Atmosphere & Environment (Clayton, VIC, Australia, a.gunn@monash.edu), ⁷Texas A&M University Department of Geology & Geophysics (College Station, TX, martindanika13@tamu.edu), ⁸Texas A&M University Department of Geology & Geophysics (College Station, TX, avivlee@tamu.edu), ⁹Stanford University Department of Earth and Planetary Sciences (Stanford, CA, mlapotre@stanford.edu).

Introduction: Sand covers vast areas of Mars' surface and deposits interpreted as aeolian in origin have been identified in situ and remotely across Mars [1]. However, the link between the surface sediment transport system that forms dune fields and the mechanisms that control accumulation and preservation of martian aeolian deposits remains poorly defined [1,2]. Explicitly linking these systems would increase the geologic context and accuracy of climate and environment interpretations based on ancient aeolian deposits [1,2,3].

On Mars, impact craters are primary sedimentary basins where aeolian deposits form, generally due to a spatial decrease in potential saturated sand flux across the crater rim as wind stresses drop [3]. This generalization belies the complexity of dune fields in crater basins, which vary significantly in size, shape, and position in the crater due to boundary conditions affecting the winds and transport through the crater. In turn, these factors affect where potential accumulation occurs and the architecture of the accumulation.

Our objectives were to identify where aeolian sediment is likely to accumulate in impact craters on Mars, explain why it accumulates there, and constrain sediment residence time at these locations. We achieved these objectives by simulating near-surface winds, computing sediment drift potential and derivatives, and synthesizing our analyses to estimate accumulation rates, dune migration rates, and surface residence time at Herschel Crater.

Methods: We used the mesoscale Mars Weather Research and Forecasting Model (MarsWRF) [4] to simulate atmospheric conditions and near-surface shear velocity at Herschel Crater for 10 sols in each of 12 seasons (30° steps in solar longitude) with instantaneous measurements every 3 hours. We calculated flux potential based on these simulations [5,6,7,8]. Time-averaged net saturated flux, q , was calculated assuming median grain diameter, $d=200\ \mu\text{m}$ [9], and grain density, $\rho=3200\ \text{kg m}^{-3}$ [10]. Sediment accumulation was calculated as the sum of incoming

net flux, proportioned using the D-infinity method [11], minus the local outgoing net flux. We approximated dune migration rate as $c=q/(0.7hp)$, where h is dune height [12]. We chose $h=20\ \text{m}$ as representative of dunes in Herschel crater, as measured in High Resolution Imaging Science Experiment digital terrain models (HiRISE DTMs). We calculated the time for a dune to travel one wavelength as $t=\lambda/c$, where λ is the crest-to-crest dune wavelength. We chose $\lambda=500\ \text{m}$ as representative of dune fields in Herschel Crater, measured in HiRISE DTMs and Mars Reconnaissance Orbiter Context Camera (CTX) imagery. We approximated the time that sand in dunes has been in the crater as d/c , where d is the distance between a sand sheet and the crater rim.

Results: Our simulations predicted Herschel Crater near-surface winds (at 1.5 m height) to be 0.0-26.3 m s^{-1} (time-averaged mean 5.3). We predicted time-averaged net flux potential, q , to be 0.0-53.5 $\text{g m}^{-1} \text{s}^{-1}$ (mean 10.1). Flux ranges between 1 and 10 $\text{g m}^{-1} \text{s}^{-1}$ in dune fields, where 3 $\text{g m}^{-1} \text{s}^{-1}$ appears representative. Peak flux magnitude occurred where flow enters the crater from the north and east. We observed convergence of flux flowlines at the edges of dune fields (dark in CTX imagery) in the northeastern and eastern portions of the crater, downstream of sediment northeast of the crater (also dark in CTX imagery; Fig. 1). Flowlines tended to converge in smaller craters, where dune fields often occur. The direction of flux was generally congruent with transport direction inferred from aeolian bedforms visible in CTX imagery (e.g., barchans). Sediment may skirt around the northern crater rim rather than enter the crater [2].

We predicted sediment accumulation immediately downwind of the crater rim (Fig. 2). Dune fields occur downwind of the eastern rim, but not downwind of the northern rim. We estimated that dunes migrate at 2.1 m per Earth year (EY) and migrate one wavelength every 238.1 EY. The dune fields in the eastern and western portions of Herschel Crater were 50-90 km downwind of the rim. The sand in these dunes may therefore have

resided in the crater for $23.8\text{--}42.9 \cdot 10^3$ EY if sourced from outside the crater.

Discussion: Our estimates of sand flux, migration rate, and reconstitution times corroborate prior research [14,15,16,17]. Research using CTX imagery measured migration rates of $0.2\text{--}0.7$ m yr⁻¹, however, perhaps due to CTX image pairs having captured a period of slow migration [17]. We found that flux gradient alone is a poor predictor dune field location in Herschel Crater, likely because sediment supply was low and heterogeneous, flux was not saturated, and modern dunes are products of antecedent conditions. Flux flowlines suggest a spatial linkage between dune fields within Herschel Crater and dark sediment northeast of the crater, indicating that sediment supply is a key factor accounting for the discrepancy between observations and our predictions. We only observed dune fields where we predicted low fluxes, which suggests that locations with high sand mobility deplete sediment faster than it accumulates, a function of both wind regime and sediment supply. With our estimates, dune sand has resided in Herschel Crater on the order of 10^4 EY. This estimate is only approximate, because transport rate varies by location (Fig. 1) and bedform size [14,15], and sediment supply is unknown. Further research is needed to understand sources of sediment into Mars craters and predict sediment supply.

We conclude that dune fields in Herschel Crater occur where (1) there exists an up-wind sediment supply; (2) sediment transport vectors converge at the up-wind margin of the dune field; (3) the flux gradient is positive in the upwind portion of the dune field; and (4) sand mobility is low, allowing time to accumulate.

Acknowledgments: The work presented here is supported through the NASA Mars Data Analysis Program grant number 80NSSC21K1090 to RCE.

References: [1] Diniega et al. (2021) *Geomorphology* 380, 107627. [2] Roback et al. (2020) *Icarus* 342, 113642. [3] Gunn et al. (2022) *Geology* 50(9), 981-985. [4] Richardson et al. (2007) *J. Geophys. Res.* 112, E09001. [5] Martin, R. L. and Kok, J. F. (2017) *Sci. Adv.* 3, e1602569. [6] Gunn et al. (2022) *Nat. Commun.* 13, 2401. [7] Bagnold (1941) *Prog. Phys. Geogr.* 18(1), 91-96. [8] Gadal et al. (2020) *Geophys. Res. Lett.* 47, e2020GL088919. [9] Swann et al. (2020) *Geophys. Res. Lett.* 47, e2019GL084484. [10] Almeida et al. (2008) *PNAS* 105(17), 6222-6226. [11] Tarboton (1997) *Water Resour. Res.* 33(2), 309-319. [12] Hayward et al. (2007) *USGS OFR 2007-1158*. [13] Fenton (2020) *Icarus* 352, 114018. [14] Rubanenko et al. (2022) *Authorea* preprint, DOI: 10.22541/essoar.167169649.93488411/v1. [15] Bridges et al. (2012) *Nature* 485, 339-342.

[16] Chojnacki et al. (2019) *Geology* 47(5), 427-430.

[17] Davis et al. (2020) *Earth Space Sci.* 7, e2019EA000874.

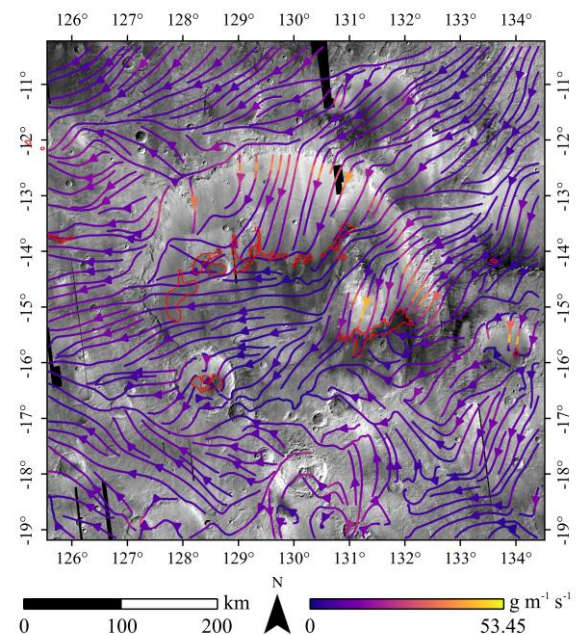


Figure 1. Time-averaged net flux potential flowlines at Herschel Crater, colored by flux magnitude, over CTX imagery. Dune fields are outlined in red [11, 12], and other dark-hued areas are associated with protodunes, sand sheets, and wind streaks.

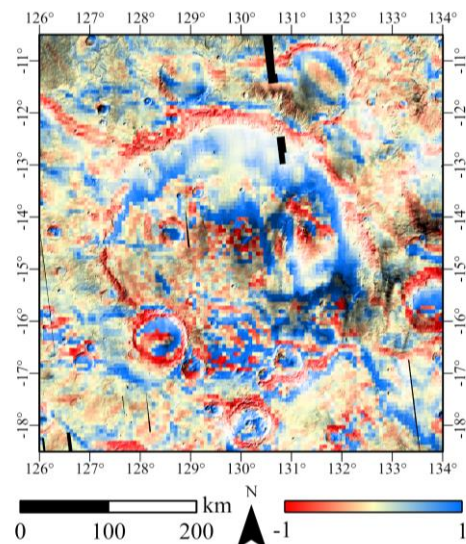


Figure 2. Normalized net saturated flux gradient at Herschel Crater, overlain on CTX imagery. Accumulation is predicted where >0 (influx $>$ outflux). Flux gradient was normalized by the local net flux magnitude to visualize spatial patterns of accumulation in areas of both high and low flux magnitude.